Volume 14 | Number 17 | 7 May 2018 | Pages 3211–3424

Soft Matter

rsc.li/soft-matter-journal

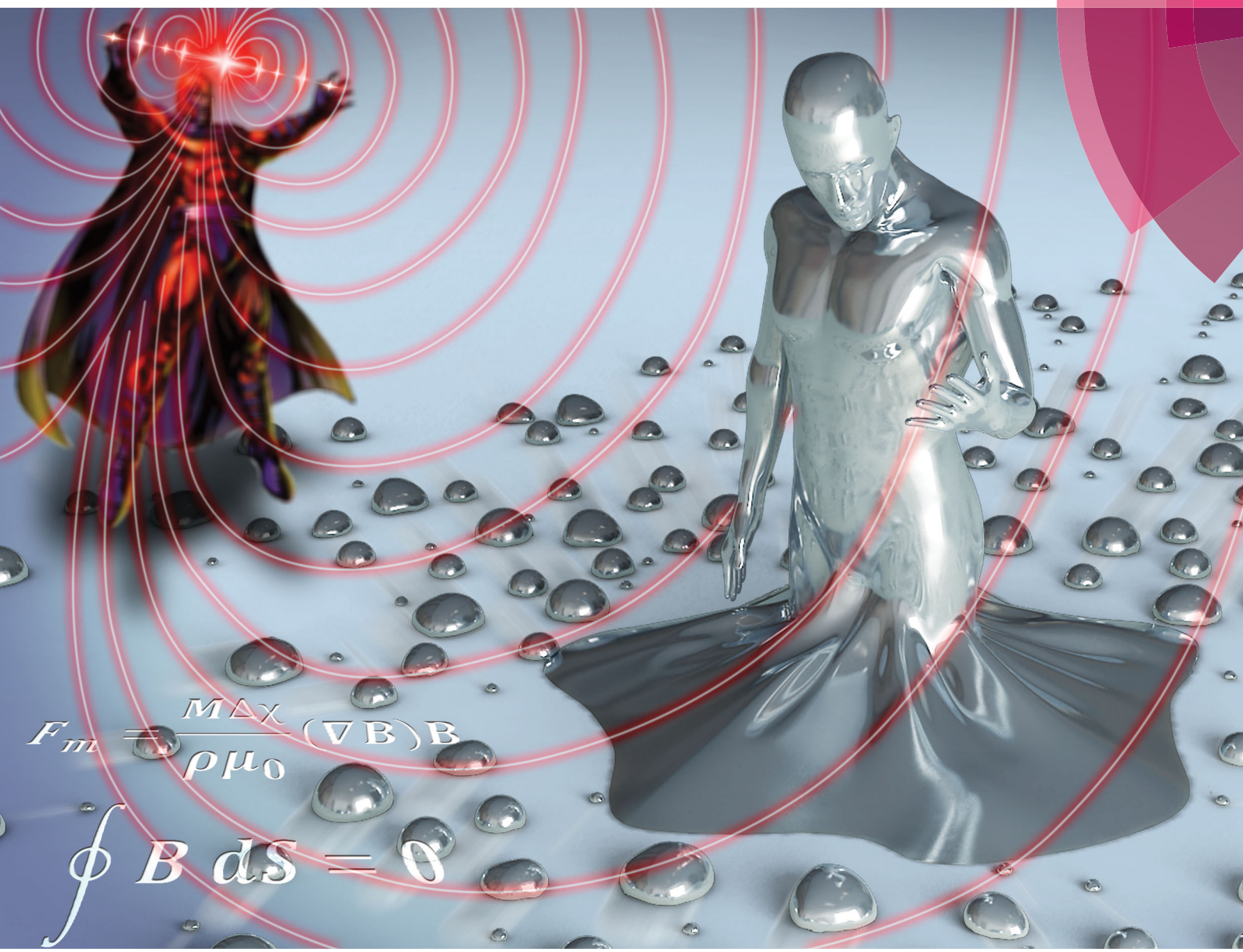

ISSN 1744-6848

ROYAL SOCIETY OF CHEMISTRY

PAPER
Feng Xu *et al.*
Magnetic steering of liquid metal mobiles

Soft Matter

PAPER

View Article Online
View Journal | View Issue

Cite this: *Soft Matter*, 2018, **14**, 3236

Magnetic steering of liquid metal mobiles†

Hao Liu,[ab] Moxiao Li,[bc] Yuhui Li,[ab] Hui Yang,[d] Ang Li,[e] Tian Jian Lu,[bcf] Fei Li[ab] and Feng Xu *[ab]

Received 7th January 2018,
Accepted 20th February 2018

DOI: 10.1039/c8sm00056e

rsc.li/soft-matter-journal

Gallium-based liquid metal has captivated exceptionally keen interest in recent years since it remains in the liquid phase at room temperature and thus conforms to the surrounding medium. Meanwhile, such morphing capability can be tuned *via* altering the oxide layer on the surface of the liquid metal, which further triggers enthusiasm for investigating its locomotion. In this study, we proposed a magnetic actuation scenario for steering liquid metal locomotion in an easily accessible and highly directed manner. The soft mobile composed of liquid metal performed satisfyingly in locomotion and assembly tasks in various circumstances (on a solid surface and in a water environment). Furthermore, promising applications as switches for logic circuits and carriers for cargo transfer, as well as motors for vessel cleaning were also demonstrated, revealing the versatility of such liquid metal mobiles.

1. Introduction

Soft materials, including but not restricted to liquids, gels and polymers, have been captivating unprecedented research interest and experiencing extensive applications in the most cutting-edge areas (like tissue engineering, flexible electronics and soft robots) over the past few decades.[1–7] Among the huge variety of soft materials, gallium-based liquid metal has recently attracted increasing attention due to its unique properties that combine liquid-like fluidity and metal-like electrical conductivity.[8–12] The secret behind such uniqueness is that the liquid metal has a remarkably low melting point ($\sim$15.5 °C),[13] so it can remain in the liquid phase at room temperature and deform its shape to the surroundings. Intriguingly, the deformation feature of the liquid metal is tunable *via* modifying the surface of the liquid metal. Specifically, a thin oxidized layer (*i.e.*, gallium oxide) instantaneously forms on the surface of the liquid metal when exposed to air. The solid oxide skin confines the liquid metal and helps the alloy to retain a desired static configuration without the need for any external structural support.[14] On the other hand, the gallium oxide layer can be crumpled and even removed under mechanical, chemical or electrical stimuli,[13,15,16] which consequently facilitates the ready and smooth flow of the liquid metal. That is to say, the morphology and motion of the liquid metal can be manipulated according to the removal of the gallium oxide layer. This interesting phenomenon of the liquid metal is inspiring for the design of novel mobile machines for practical applications far beyond the traditional uses like drug delivery and water purification.[17–19]

The directed control of motion is a primary requirement for realizing liquid metal mobile objects. The current strategies for steering liquid metal motion are mostly based on electrohydrodynamics and involve the harnessing of a proper voltage to remove the oxide layer formed on the surface of the liquid metal, thus enabling transformation and movement of the alloy.[15,16,20,21] However, these methods are associated with several limitations, such as the requirement of shaped capillaries and molds[15,16] and the skillful arrangement of electrode geometries for directed motion.[21] Although the self-powered liquid metal motor proposes a useful paradigm for auto locomotion,[22] it merely rotates around randomly and needs specific geometrical channels to achieve directional motion. In comparison, the use of magnets has been proven to offer a feasible route for the well-directed driving and assembly of functional soft blocks.[23–25] Building magnetic marbles through the coating of magnetic iron particles on the surface of liquid metal droplets turned out to be feasible for the on-demand magnetic manipulation of a liquid metal.[26–28] Additionally, a conceptual application of electrical switching was realized using the as-proposed magnetic liquid metal marbles with the help of shape-confined microfluidic channels.[27] A recently reported dual-mode actuation (*i.e.*, magnetic-electrical actuation)

[a] *The Key Laboratory of Biomedical Information Engineering of Ministry of Education, School of Life Science and Technology, Xi'an Jiaotong University, Xi'an 710049, P. R. China. E-mail: fengxu@mail.xjtu.edu.cn*
[b] *Bioinspired Engineering and Biomechanics Center (BEBC), Xi'an Jiaotong University, Xi'an 710049, P. R. China*
[c] *State Key Laboratory for Strength and Vibration of Mechanical Structures, School of Aerospace, Xi'an Jiaotong University, Xi'an 710049, P. R. China*
[d] *School of Life Sciences, Northwestern Polytechnical University, Xi'an 710072, P. R. China*
[e] *Key Laboratory of Shaanxi Province for Craniofacial Precision Medicine Research, College of Stomatology, Xi'an Jiaotong University, Xi'an 710049, P. R. China*
[f] *MOE Key Laboratory for Multifunctional Materials and Structures, Xi'an Jiaotong University, Xi'an 710049, P. R. China*

† Electronic supplementary information (ESI) available. See DOI: 10.1039/c8sm00056e

turned out to be capable of flexibly and controllably steering a liquid metal droplet, in which a nickel cap is electroplated on the surface of the liquid metal to drag the nickel/liquid metal mobile as a whole under magnetic stimuli.[29] Nevertheless, the covering nickel is solid and hard, in contrast to the liquid metal in softness, and so there are potential adverse impacts to some applications of liquid metal mobiles in confined spaces where shape-adaptability is favored. Another unfavorable hurdle associated with this strategy is that the inevitable employment of an electroplating procedure unnecessarily complicates the whole operation process and further undermines the simple and easily accessible features of magnetic manipulation. In addition, most of the current studies on manipulating liquid metal are carried out within sodium hydroxide (NaOH) solution since it can remove the oxide layer and thus facilitate the liquid metal performing like a fluid.[16,20,22] However, the dependence on NaOH solution may hinder its applications for various practical purposes. Therefore, there is still an unmet demand for a versatile scenario for steering liquid metal motion in a straightforward, directed and controllable manner.

Herein, we introduce a versatile approach that employs magnetic force for steering liquid metal (eutectic gallium indium) mobiles in an easily accessible, precisely targeted and highly controllable way. Each liquid metal droplet (mobile) encapsulates several microsized steel beads (as engines) that can be preserved in the droplet thanks to the thin, gallium oxide layer covering the surface of liquid metal, which thus enables the droplets to move and assemble with each other in response to a permanent magnet. It is noted that the liquid metal mobiles can operate both in water and on a solid (paper) substrate, making them versatile for different working

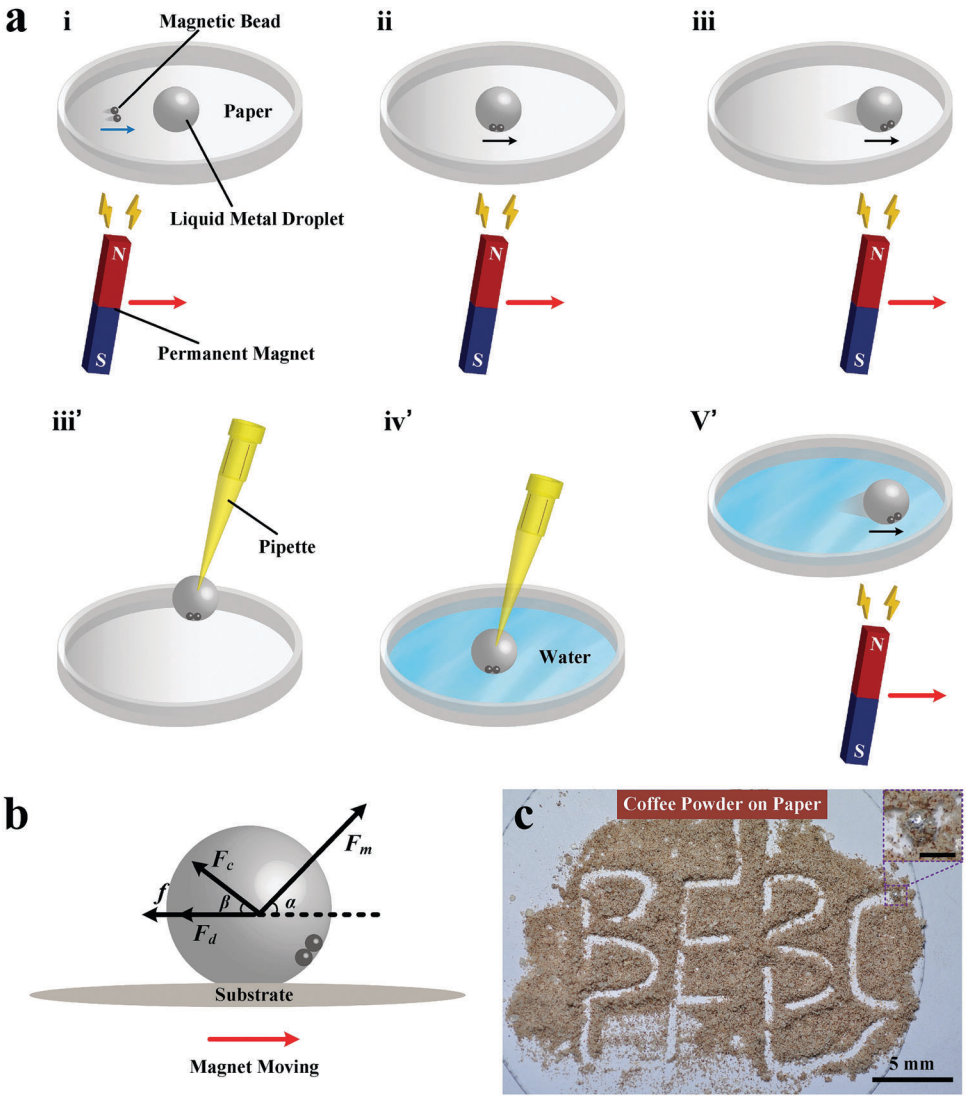

Fig. 1 Magnetically steered liquid metal mobiles. (a) Schematic illustrating the directed magnetic steering process of the liquid metal droplet (mobile). (b) Force diagram of a moving liquid metal droplet under magnetic drive. F_m, F_c, F_d and f indicate the magnetic driving force, the capillary force between the magnetic beads and the liquid metal droplet, the drag force from ambient fluids (air or water) and the friction from the substrate, respectively. (c) Specific pattern of text "BEBC" arising from the magnetically driven shuttling of a liquid metal mobile through coffee powder distributed on a piece of printing paper. The inset presents an enlarged photograph of the liquid metal mobile after shuttling. Scale bar is 1 mm.

circumstances. Furthermore, the favorable performances in the healing of paper-based flexible electronics, cargo transfer and vessel cleaning are demonstrated to reveal the huge application value of the magnetically steered liquid metal tactic for soft mobile design.

2. Materials and methods

The liquid metal material used for all of the experiments presented in this paper was eutectic gallium indium (Sigma Aldrich, USA). The magnetic driving force was supplied by a permanent bar magnet (length × width × height: 60 × 13 × 10 mm). To realize certain driving velocities of the magnet, it was attached to the sliding block of a digitally controlled moving platform (Y90TA, JYGD Instruments, China). The magnet could then move at the same velocity as the movement of the sliding block. Spherical steel beads made of carbon steel were purchased from Xinda Steel Products, China, and beads with three different sizes (diameters of 0.35, 0.5 and 0.8 mm) were used in the experiment. The magnetic flux density applied to the liquid metal droplet was measured using a gauss meter (Model 1800, Ch-Hall Electronic Devices Co., Ltd, China). Videos were recorded using a digital camcorder (FDR-AX30, Sony, Japan) to present the detailed experimental observations and the snapshots demonstrated in each figure were extracted from the corresponding videos.

3. Results

3.1 Preparation of the liquid metal mobile

The fabrication process of the magnetically steered liquid metal mobiles is depicted in Fig. 1a. The process began with encapsulation of the microsized steel beads into liquid metal droplets on a sheet of printing paper with the horizontal movement of a permanent bar magnet (i and ii). Subsequently, the beads continued to move until reaching the droplet boundary, and they further induced on-site droplet deformation due to the applied magnetic force. In this way, the liquid metal droplet underwent steady locomotion on the solid surface subjected to the magnetic field (iii). The liquid metal mobiles also showed capability of performing in water through successive procedures of transferring the steel bead-containing droplet into a water environment and driving with the magnet (iii′–v′). In the proposed scenario, movement of the liquid metal droplet is theoretically determined by the dynamic equilibrium among the magnetic driving force (F_m) operating on the beads, the friction (f) from the substrate surface, the drag force (F_d) from the surrounding medium (air or liquid), as well as the capillary force (F_c) arising from the droplet deformation (Fig. 1b). Thanks to the solid, thin oxide layer of gallium oxide covering the surface of the liquid metal, the steel beads can be held inside the liquid metal droplet and drag the droplet to move in any direction under magnetic actuation. In addition, since gallium is easily oxidized to produce gallium oxide, this oxide layer instantaneously and continually forms on the surface of the liquid metal as soon as the liquid metal is exposed to the air.[13] So the oxide can be dense and the effect of possible fracture of the oxide layer (only existing for a transient period of time) to the macroscopic movement of the liquid metal droplet is minimal and can be neglected. Meanwhile, the capillary force is produced when the steel beads are magnetically driven away from the droplet, pressing against the boundary of the liquid metal droplet. This obstruction from the liquid metal itself also contributes to preventing the beads from being extracted out. Under this mechanism, the liquid metal droplet can realize highly directed motion, as demonstrated by the specific pattern of ''BEBC'' induced by the accurate magnetic locomotion of the liquid metal droplet on a coffee powder-coated paper surface (Fig. 1c). Additionally, the magnetically-actuated liquid metal droplet locomotion can also be induced in a confined space, and this is clarified by the fact that the liquid metal droplet (~2 mm in initial diameter) can proceed smoothly and swiftly through a solid narrow channel (1 mm in width) by ingeniously deforming to adapt its morphology to the ambient channel wall (Movie S1 and Fig. S1, ESI†).

3.2 Directed locomotion of liquid metal mobiles steered by magnets

The capability of directed locomotion is further validated by uniform movement with constant velocity under magnetic actuation, as presented by driving a 5 μL liquid metal droplet with average velocities of 60 and 65 mm s^{-1} on paper and in water, respectively (Fig. 2a and b and Movie S2, ESI†). To study the magnetic actuation performance, the actual velocities of liquid metal droplets with diverse volumes (5, 10, 15 and 20 μL) at various magnet driving velocities (0–70 mm s^{-1}) were investigated both on paper and in water (Fig. 2c–f). The experimental results imply that small droplets (*e.g.*, 5 μL) exhibit stable drive by the magnetic field with practical velocities close to those of the moving magnet (Fig. 2c), whilst droplets with larger volumes tell remarkably different stories. Specifically, locomotion of the 10 μL droplet reveals nearly perfect agreement with the theoretical velocities provided by the magnet for slow driving. But the droplet surprisingly slows down as the driving magnet accelerates to 50 mm s^{-1}, and finally stops on the paper substrate, accompanied with bead extraction, at a driving velocity of 56 mm s^{-1}. However, for the test in water, the droplet continues to move steadily with negligible impact from the increase of driving velocity (Fig. 2d). The 15 μL case resembles the observation for the 10 μL droplets, however with one significant distinction that the corresponding cutoff velocity at which the droplet fails to be driven on paper shifts to approximately 20 mm s^{-1} (Fig. 2e). As for the 20 μL instance, the droplet remains still on paper for each tested driving velocity, and bead extraction behavior occurs in water at magnet driving velocities higher than 63 mm s^{-1} (Fig. 2f).

The underlying mechanism of these phenomena can be explained by the balance of mechanics among the aforementioned forces applied to the liquid metal mobile, namely the magnetic force (F_m), the friction force (f), the drag force (F_d) and the capillary force (F_c), which collaborate to govern the

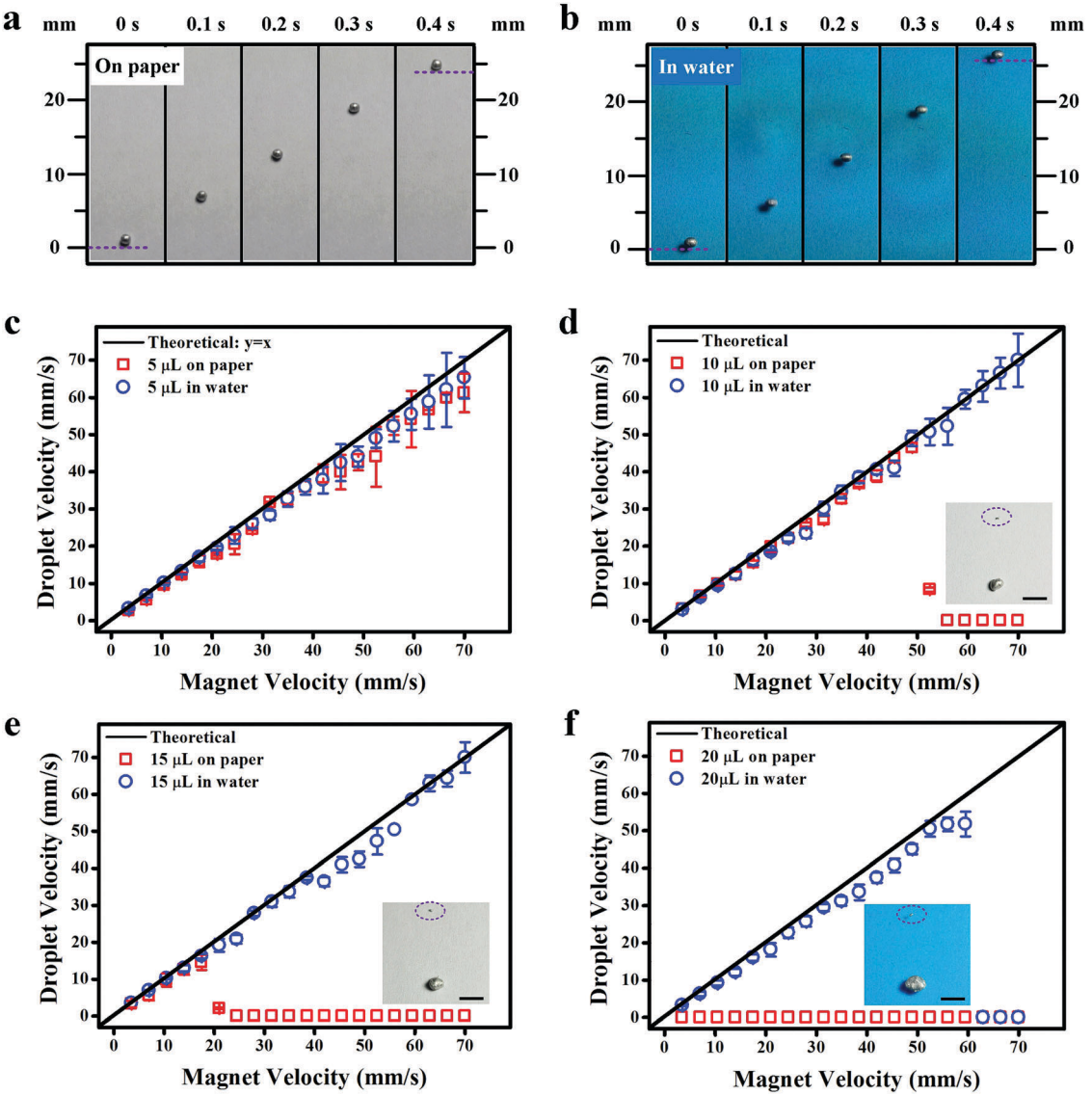

Fig. 2 Directed locomotion of liquid metal mobiles *via* magnetic steering. (a and b) Sequential snapshots of the 5 μL liquid metal droplet locomotion on paper (a) and in water (b) with a magnetic driving velocity of 70 mm s^{-1}. (c–f) Actual velocities of liquid metal droplets with diverse volumes of 5 (c), 10 (d), 15 (e) and 20 μL (f) on paper and in water, as a function of the magnet driving velocity. The insets show the bead extraction phenomenon with purple dotted ellipses indicating the extracted beads on paper (d and e) and in water (f). Scale bars are 5 mm. Error bars represent standard deviation (N = 3).

magnetic manipulation system. Specifically, the total magnetic force experienced by the steel beads in the liquid metal can be obtained by[30]

$$F_m = \frac{M\Delta\chi}{\rho\mu_0}(\nabla B)B \quad (1)$$

where M is the total mass of the steel beads; ρ is the density of the steel beads; $\Delta\chi$ is the difference in magnetic susceptibility between the steel beads and the liquid metal; B and ∇B are the magnetic flux density and magnetic field gradient, respectively. When the steel beads are close to the inner boundaries of the liquid metal droplet, they will press against the droplet, thus generating a capillary force. Considering the bead cluster as a single equivalent sphere, the capillary force which preserves the beads within the droplet can be estimated using the outer circumference of the sphere.[31]

$$F_c = \sqrt[3]{6\pi^2\gamma\left(\frac{M}{\rho}\right)} \quad (2)$$

where γ is the surface tension of the liquid metal–air interface. When the droplet is moving, the drag force is defined as:[32]

$$F_d = \frac{1}{2}\rho_s v^2 c_d A \quad (3)$$

where c_d is the drag coefficient, which depends on the Reynolds number Re for a certain body shape, ρ_s is the density of the surrounding fluid (air/water), v is the velocity of the liquid metal droplet, and A is the reference area of the droplet, which

depends on its shape. Considering the horizontal direction, we conclude a force balance equation presented as below:

$$F_m \cos\alpha - F_c \cos\beta - f - F_d = 0 \quad (4)$$

where α represents the angle between the magnetic field vector and the horizontal direction, and β indicates the angle between the capillary force and the horizontal direction. In the magnetically actuated droplet locomotion, the magnetic force is the sole driving force whilst the friction and drag forces collaborate to cause the main hindrance. The steel beads can be preserved within the liquid metal droplet and pull the droplet to move when the magnetic driving force overcomes the friction but is still less than the maximum value of the capillary force. But due to the friction between the liquid metal droplet and the substrate, the liquid metal cannot perform instantaneous movement as the magnet moves. Instead, a time delay exists between movements of the magnet and the droplet (Fig. S2, ESI†). Besides, the existence of the oxide layer on the liquid metal surface plays an additional part in the magnetically-driven droplet locomotion. Specifically, a solid oxidized shell (*i.e.*, gallium oxide) spontaneously forms and covers the outside of the liquid metal, stabilizing the droplet to retain unique morphologies and keep the encapsulated beads from getting out. Nevertheless, from eqn (1) and (2), it can also be notably deduced that the magnetic force will exceed the capillary force when M/ρ (*i.e.*, the amount of steel beads) is exceptionally large, and the beads will consequently be extracted out. Therefore, two significantly different phenomena of steady drive and bead extraction can be clearly observed as displayed in Fig. 2c–f. Theoretically, bead extraction would take place when the friction force (f) and the maximum hindrance force of the liquid metal (F_h) are respectively larger than the maximum magnetic force ($F_{m,max}$).

$$f > F_{m,max} \quad (5)$$

$$F_{h,max} > F_{m,max} \quad (6)$$

Here, F_h is defined as the sum of the capillary force from the liquid metal itself and the obstruction from the oxide layer on the surface of the liquid metal (F_o). Specifically, F_o is the counterforce when the steel beads are magnetically driven to reach the boundary of the liquid metal and press its oxidized surface. So eqn (6) could be rearranged as:

$$(F_c + F_o)_{max} > F_{m,max} \quad (7)$$

In addition to the M/ρ ratio, some other factors like magnet driving velocity and droplet volume are found to impact the movement state as well. The liquid metal droplet can be steadily driven by slowly moving the magnet, whilst bead extraction will take place at higher velocities, which can also be manifested by the downward trend of the maximum droplet volume that can be driven (V_{max}) as the driving velocity rises (Fig. S3, ESI†). Similarly, with increasing volume of the liquid metal droplet, the driving of the droplet by the magnetic force becomes increasingly arduous, and the steel beads can separate the liquid metal droplet into two smaller blobs and may even be dragged out of the droplet body. Besides, it is suggested from the experimental observations that the size of the beads additionally impacts on the droplet motion (Fig. S4, ESI†). In detail, the beads used in this test are of 3 different sizes (diameters of 0.35, 0.5 and 0.8 mm) but have the same density, thus a larger size and more encapsulated beads will lead to increased bead mass (M), which further affects the liquid metal motion status. The magnetic driving force is also affected by the magnetic flux density applied to the liquid metal droplet, which varies with the change in the distance between the substrate and the magnet (Fig. S5, ESI†). In this work, the magnet–substrate distance was 1 mm. Therefore, we can flexibly manipulate the movement state of the liquid metal droplet, such as switching steady drive into bead extraction, *via* tuning the driving velocity, magnetic force (the size and number of beads, and the distance between the substrate and the magnet) and volume of the droplet.

3.3 Directed assembly of liquid metal mobiles steered by magnets

Apart from the oriented locomotion of a single droplet, the feasibility of assembling several liquid metal blobs with the proposed magnetic actuation strategy was also studied (Fig. 3). Theoretically, under appropriate magnetic stimulation, the encapsulated beads tend to pull the liquid metal droplets together to the magnet site where the droplets deform and fuse once they are in contact with each other (Fig. 3a). Fig. 3b and c reveal the sequential assembly procedures of two 5 μL liquid metal droplets (each with 2 steel beads encapsulated) carried out on paper (Fig. 3b) and in water (Fig. 3c) by manually swaying and rotating a permanent bar magnet under the Petri dish (also shown in Movie S3, ESI†). The whole assembly process occurs swiftly (less than 20 seconds) and the fused droplet satisfyingly moves in an intact and smooth manner with magnetic manipulation (Movie S3, ESI†). However, the as-assembled droplet demonstrates ellipsoid geometry instead of a perfectly spherical profile in water (Fig. 3c(iv)), which can be ascribed to the stabilizing solid oxide layer formed on the liquid metal droplets, as well as the synergy of friction of the liquid metal–Petri dish wall interface and liquid metal–water interface. To further simplify the assembly approach, we magnetized a ubiquitous pin with a permanent bar magnet and adopted such an unsophisticated tool to provide the required magnetic field for assembly (Fig. 3d and Movie S4, ESI†). A proof of concept was conducted by successfully assembling 3 blobs into one, and the merged liquid metal droplet presents surprisingly robust adhesion to the magnetized pin (Movie S4, ESI†) owing to the strong magnetic force applied to the encapsulated bead cluster (as denoted by the red dotted circle in Fig. 3d(v)).

3.4 Magnetically steered liquid metal mobiles for healing paper-based electronic circuits

Liquid metal is well known for its inherently high electrical conductivity,[33] and hence has been shown to have potential applications in flexible electronics. Coupled with the presented

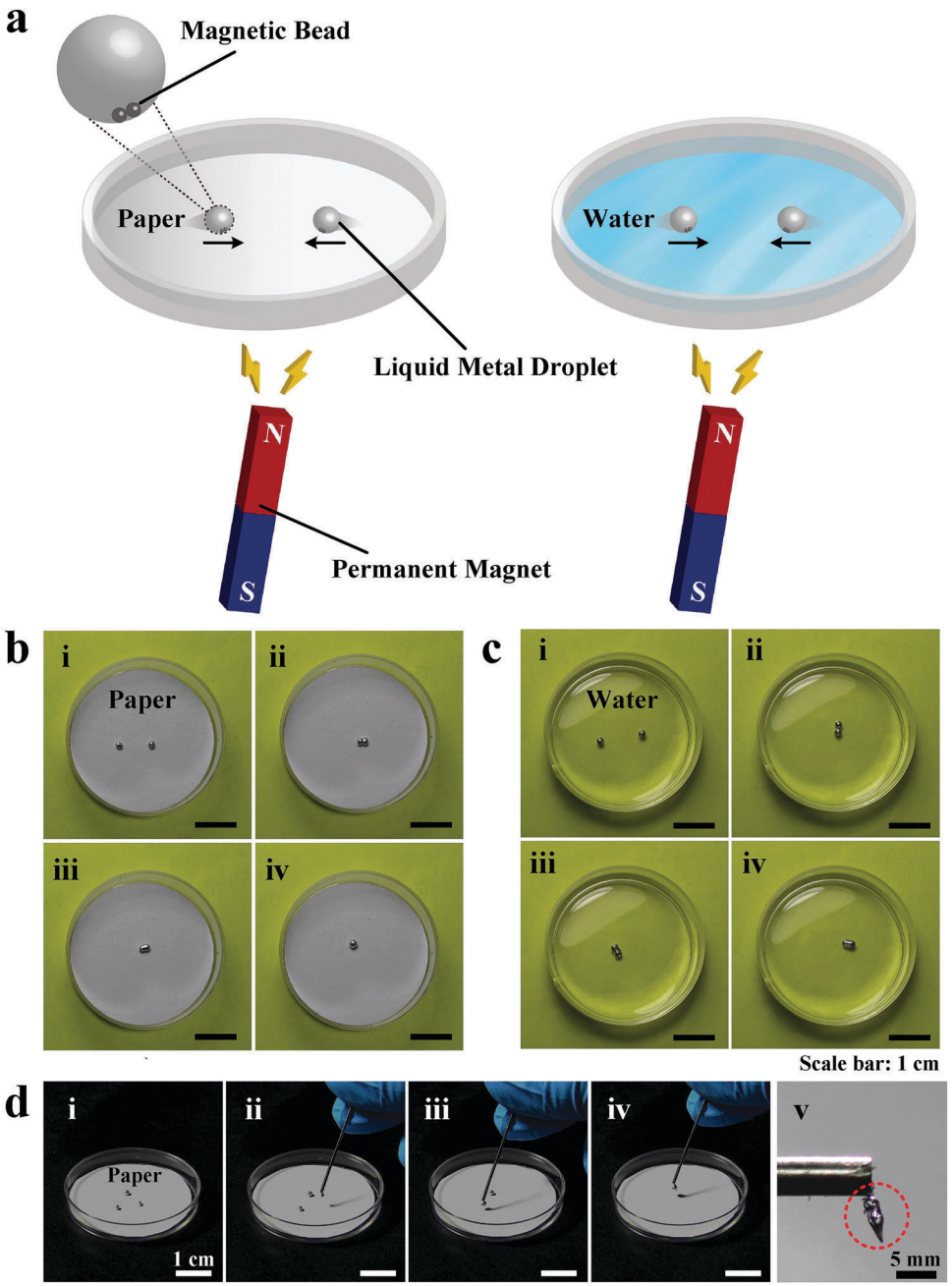

Fig. 3 Directed assembly of liquid metal mobiles *via* magnetic steering. (a) Schematic diagram of the directed magnetic assembly of liquid metal droplets. (b and c) Digital photographs describing the directed assembly of two liquid metal droplets on paper (b) and in water (c) under magnetic manipulation. (d) Simplified assembly of liquid metal droplets with a magnetized pin (i–iv). (v) A cluster of magnetic beads after casting off the assembled droplet (shown in iv), as denoted by the red dotted circle.

magnetic actuation paradigm, we can further use the soft liquid metal mobiles for electronics purposes. For instance, the mobiles can be designated as switches for reconnecting open circuits, which are of great use in the electronics industry (Fig. 4). As schematically elucidated in Fig. 4a, copper electrodes were meticulously arranged and connected to a power supply, light emitting diodes (LEDs) L_1 (red) and L_2 (yellow) were introduced to respectively indicate the connectivity of AND and OR logic circuits, and liquid metal mobiles in starting positions A and B could be driven by magnets to fill blanks between electrodes and further connect the corresponding logic circuit as denoted by LED emission. The situation can be equivalent to the operating block of an AND-OR droplet logic gate, where positions A and B function as inputs ("1" for the presence of droplets and "0" for the absence of droplets), while LEDs L_1 and L_2 represent output signals ("1" for lighting up and "0" for remaining dark) (Fig. 4b). In experimental realizations, liquid metal mobiles were initially placed at input sites,

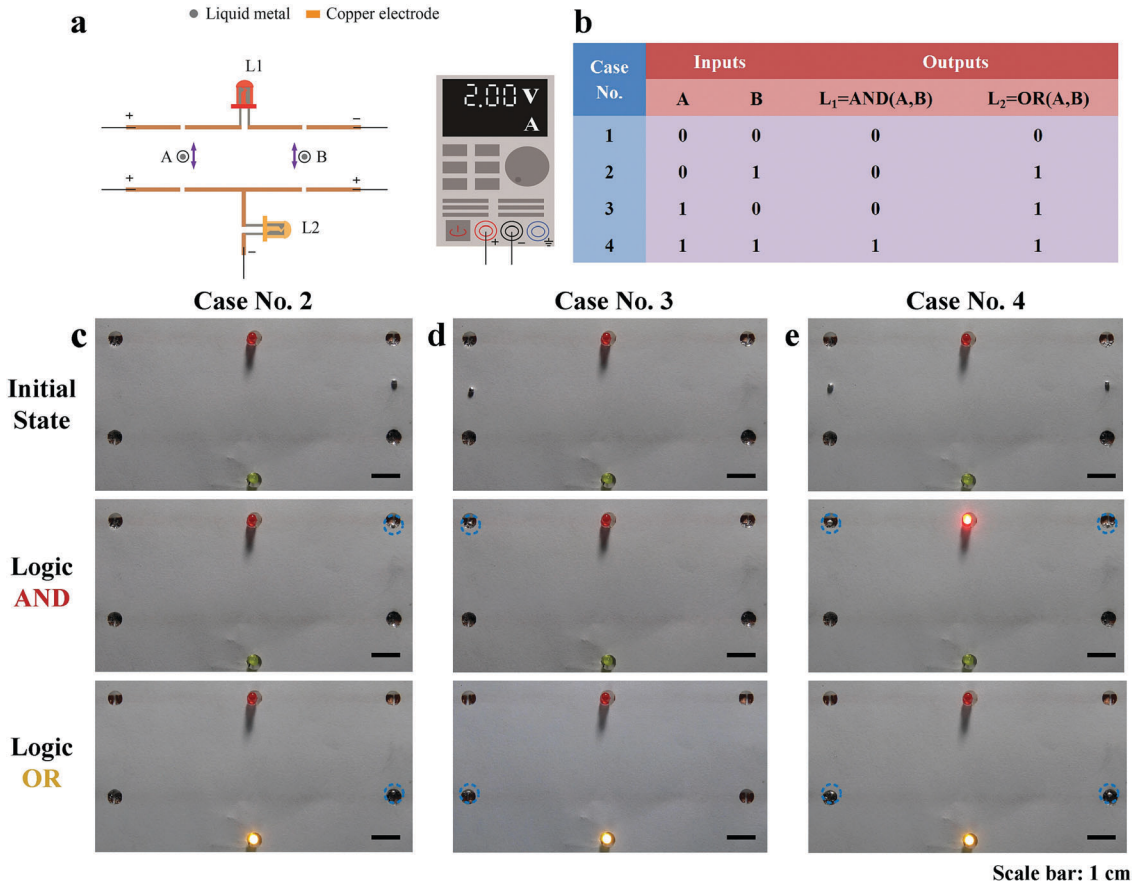

Case No.	Inputs		Outputs	
	A	B	L_1=AND(A,B)	L_2=OR(A,B)
1	0	0	0	0
2	0	1	0	1
3	1	0	0	1
4	1	1	1	1

Fig. 4 Application as switches for a paper-based logic gate circuit. (a) Schematic of the logic switching functionality of magnetically steered liquid metal mobiles. The LEDs, L_1 as logic AND and L_2 as logic OR, illuminate (marked as output "1") or dim (marked as output "0") as responses to the presence (marked as input "1") or absence (marked as input "0") of liquid metal mobiles on sites A and B. (b) Truth table of the logic gate circuits. (c–e) Experimental demonstrations of logic cases No. 2–4, respectively. The blue dotted circle in each image indicates the final position of the liquid metal mobile for connecting circuits.

followed by magnetic locomotion to output ports where the logic circuits were disconnected. The droplet subsequently reconnected the open circuit by gluing the isolated copper electrodes together, as reflected by the LED illumination (Fig. 4c–e and Movie S5, ESI†). In other words, the liquid metal mobile is assigned here as a switch to turn on the logic gate circuit.

3.5 Magnetically steered liquid metal mobiles for cargo transfer

Miniaturized motors capable of transferring and releasing cargo are attracting great interest in research communities including for soft robots, drug delivery and environmental pollution treatment.[34–36] Therefore, to investigate the feasibility of the liquid metal mobile for cargo transfer applications, we designed a proof-of-concept demonstration as illustrated in Fig. 5a (Movie S6, ESI†). Specifically, we pipetted cargo (yellow wax flakes)-laden gelatin solution onto a liquid metal mobile and the cargo carrier was fabricated after the curing of gelatin at room temperature for 10 min. The carrier loaded with cargo was then guided to the destination under magnetic steering (Fig. 5b). A subsequent heating procedure (10 min, 37 °C) was carried out to melt the covered gelatin hydrogel and unload the cargo (Fig. 5c). What deserves to be noted is that the releasing period of the cargo can be flexibly tuned *via* the use of different concentrations and volumes of the gelatin hydrogel. After cargo unloading, the liquid metal mobile (cargo carrier) could be recalled and magnetically driven to the starting position to await the next task (Fig. 5d).

3.6 Magnetically steered liquid metal mobiles for vessel cleaning

Nowadays, incidence of cardiovascular diseases (*e.g.*, atherosclerosis) is unexpectedly experiencing a rising trend. One main pathogenesis of such diseases lies in the blockage of blood vessels induced by cholesterol deposits, making cleansing blood vessels of cholesterol deposits quite crucial for maintaining health. Therefore, we show another application aspect of the as-designed magnetic-actuated liquid metal mobile in blood vessel cleaning, benefiting from the biological benignancy of liquid metal that has been validated by deploying it as a carrier for targeted drug delivery.[37] Fig. 6a demonstrates the prototype mechanism for blood vessel cleaning, which is the application of a steel bead-encapsulated liquid metal droplet

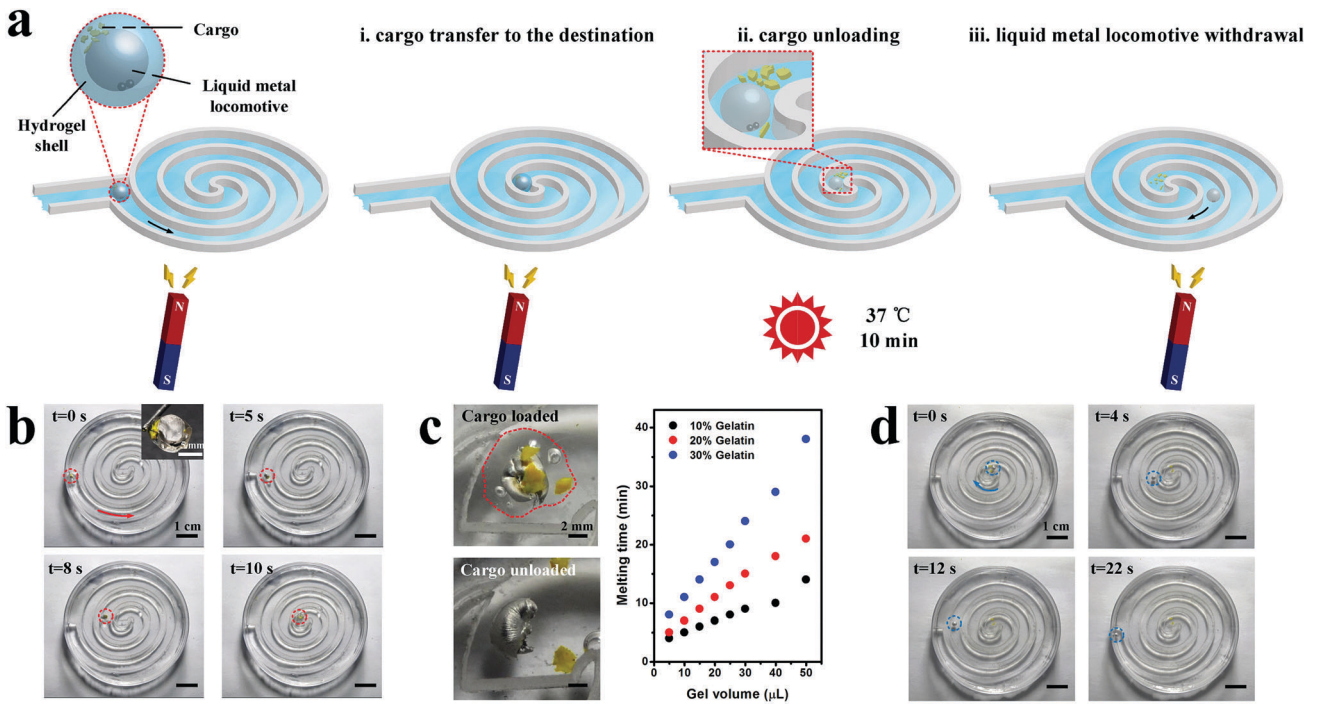

Fig. 5 Application as a cargo transfer carrier. (a) Schematic of the cargo transfer process in a spiral channel with the liquid metal mobile. (b) Snapshots of the transfer process with the liquid metal carrier (red dotted circle). The inset is the digital photograph of the cargo transfer carrier based on covering cargo (yellow)-laden gelatin hydrogel (transparent) onto the surface of the liquid metal mobile (grey). (c) Left: Digital photographs of the cargo unloading process as a result of the melting of the hydrogel at 37 °C. The red dotted line in the top photo outlines the profile of the covered hydrogel. Right: Cargo unloading time (hydrogel melting time) with different concentrations and volumes of hydrogel. (d) Snapshots of the withdrawal of the liquid metal mobile (blue dotted circle) after unloading the cargo to demonstrate its reusability.

(as shown by the grey dotted circle) as the motor to break up waste residuals (as depicted by the yellow dotted ellipse) stuck in a vessel. The pseudo blood vessel was made of a hollow-structured polyacrylamide hydrogel filled with red dyed water as blood, and wax flakes chopped off from a yellow wax pen were immersed into it to mimic cholesterol residuals. In the cleaning process, the liquid metal motor is stimulated by magnetic force to move to the stuck site and then collapse through the deposit submerged in the vessel with distinguishable morphology change (Fig. 6b–f and Movie S7, ESI†).

4. Discussion

As we have demonstrated, the steel bead-encapsulated liquid metal droplets, namely liquid metal mobiles, implement directed

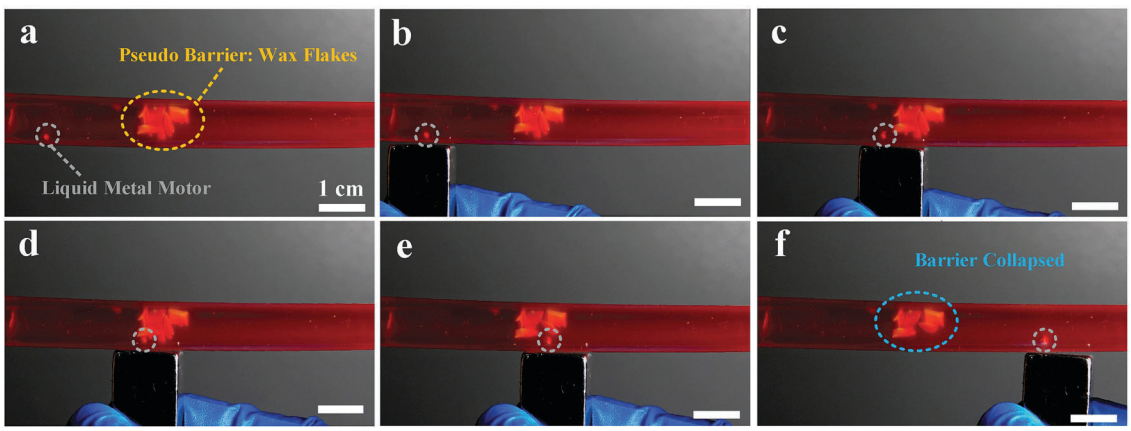

Fig. 6 Application as vessel cleaning motor. (a) Digital photograph of a mimetic blood vessel blocked with deposits, shown by the yellow dotted ellipse. (b–f) Snapshots of the cleaning process realized by the magnetic drive of a liquid metal motor (grey dotted circle) to break up waste residuals, as depicted by the blue dotted ellipse in (f).

locomotion and assembly with the guidance of a magnetic field. Currently reported liquid metal locomotion scenarios mainly focus on locomotion in an aqueous environment and circumvent that on solid substrates due to the potential for the liquid metal to adhere to the solid surfaces. However, such dependence on aqueous conditions may greatly limit the vast application perspective for liquid metal mobiles. We herein validate that the liquid metal mobile steered by magnets provides satisfactory performance both on solid surfaces and in aqueous surroundings, making it available and versatile for different working situations. To the best of our knowledge, this is the first demonstration of driving and assembling liquid metal both on a solid substrate exposed to air and in a pure water medium, which is promising to expand the application realm for liquid metal mobiles. The solid substrate selected for the experimental tests was commercially available printing paper due to its metallophobicity to liquid metal, as we have previously reported.[38] This favorable property hampers penetration and adhesion of liquid metal to the textured surface, thus prompting the smooth and swift movement of the liquid metal droplet on printing paper. Nevertheless, suitable solid substrates should not be limited to paper in spite of its low cost and abundant presence in daily life. Fortunately, with more studies of the interaction between liquid metal and solid surfaces (*i.e.*, wetting properties),[39] an increasing number of metallophobic substrates are promising to share the stage in the operation of liquid metal motion. For example, a hydrochloric acid-treated paper towel with superb lyophobicity against gallium-based liquid metal may be an appropriate substrate for liquid metal manipulation and could find potential applications in microfluidics.[40] As for the manipulation in a water medium, a magnetic levitation method may be inspiring to further reinforce the currently proposed magnetic actuation scenario. Specifically, the magnet can be held above the water in air to elevate the liquid metal droplet from the bottom wall of the container and help the droplet to float in water, which shows potential to eliminate the resistive friction from the Petri dish wall and hence facilitate droplet locomotion in water.

Compared to the currently reported strategies for liquid metal locomotion and assembly (*e.g.*, through applying electrical voltage[15,16,20,21]), the as-proposed magnetic actuation route possesses some outstanding advantages. This method is cost-effective and easily accessible, since it doesn't require any specific peripheral equipment like the power supply used in some of the other reports,[15,16,20,21] and a bar magnet can simply help to realize the locomotion. Another advantage of the magnetic way is its highly controllable precision, which facilitates the liquid metal droplets being driven to and assembled at a particularly desirable position. In addition, the proposed scenario is significantly different from the recently reported electro-magnetic actuation for liquid metal manipulation with the help of electroplated, stiff nickel, which may weaken the shape-adaptable feature of the liquid metal-based soft mobile. A thin oxide layer originating from the liquid metal itself is harnessed in this article to encapsulate magnetic-responding elements, *i.e.*, steel beads, in the liquid metal droplet and the shape-adaptability can be well maintained in this way (Movie S1 and Fig. S1, ESI†).

Another aspect demanding intensive attention is that the motion state of the liquid metal mobiles can be flexibly shifted from steady locomotion to bead extraction, regardless of the surrounding environment they are assigned to. As previously described, a number of factors, including the magnetic field intensity, the driving magnet velocity, and the volume of the liquid metal droplet, as well as the size and number of beads encapsulated in the droplet, play important roles in governing the motion state of the liquid metal mobile. For instance, a specific volume of droplet moves stably following a slowly moving magnet, while the beads will probably be dragged out of the droplet once the driving magnet speeds up and the droplet accordingly stops advancing. Another case is that for a certain driving velocity, a small liquid metal droplet (*e.g.*, 5 μL) follows steady locomotion whereas a larger one (*e.g.*, 20 μL) fails to be driven as presented by bead extraction. Additionally, changing the environmental conditions may also affect the movement status of the liquid metal mobiles. An example is to put the liquid metal into an acidic or alkaline aqueous medium where the oxide layer of the liquid metal can be removed, and the maximum applied magnetic force to ensure steady movement of the liquid metal droplet should be altered accordingly. Additional attention should also be paid to the promising engagement of an electromagnet, since the tunable magnetic field it generates can be rapidly altered through modulation of the electric current in the wires winding around the magnetic core, thus facilitating precise magnetic control over the liquid metal motion. Such a feature is beneficial to some practical applications where encapsulated steel beads need to be separated from the droplet once the task is accomplished for the liquid metal mobile.

5. Conclusions

In conclusion, this study reveals that the proposed magnetic steering scenario presents a complementary and more easily accessible substitute method for realizing directed motion of liquid metal mobiles. Owing to the encapsulation of microsized steel beads (engines), liquid metal droplets (mobiles) perform highly targeted and controllable locomotion and assembly both on a solid surface and in a liquid medium subjected to the applied magnetic field. In addition, the embedded beads can be flexibly extracted out by adjusting related parameters (*e.g.*, driving velocity) when locomotion for practical purposes is done and they are no longer wanted. Furthermore, the magnetic actuation of liquid metal motion introduced here holds great potential for diverse areas including soft robotics, flexible electronics and microfluidics research in the near future.

Conflicts of interest

There are no conflicts to declare.

Acknowledgements

This work was financially supported by the National Natural Science Foundation of China (21775117, 11522219, and 11532009), the International Science and Technology Cooperation and Exchange Program of Shaanxi Province of China (2016KW-064) and the General Financial Grant from the China Postdoctoral Science Foundation (2016M592773).

References

1 M. Lutolf and J. Hubbell, *Nat. Biotechnol.*, 2005, **23**, 47.
2 A. Khademhosseini and R. Langer, *Biomaterials*, 2007, **28**, 5087–5092.
3 D.-H. Kim, N. Lu, R. Ma, Y.-S. Kim, R.-H. Kim, S. Wang, J. Wu, S. M. Won, H. Tao, A. Islam, K. J. Yu, T.-i. Kim, R. Chowdhury, M. Ying, L. Xu, M. Li, H.-J. Chung, H. Keum, M. McCormick, P. Liu, Y.-W. Zhang, F. G. Omenetto, Y. Huang, T. Coleman and J. A. Rogers, *Science*, 2011, **333**, 838–843.
4 J. A. Rogers, T. Someya and Y. Huang, *Science*, 2010, **327**, 1603–1607.
5 D. Rus and M. T. Tolley, *Nature*, 2015, **521**, 467–475.
6 N. W. Bartlett, M. T. Tolley, J. T. Overvelde, J. C. Weaver, B. Mosadegh, K. Bertoldi, G. M. Whitesides and R. J. Wood, *Science*, 2015, **349**, 161–165.
7 R. F. Shepherd, F. Ilievski, W. Choi, S. A. Morin, A. A. Stokes, A. D. Mazzeo, X. Chen, M. Wang and G. M. Whitesides, *Proc. Natl. Acad. Sci. U. S. A.*, 2011, **108**, 20400–20403.
8 M.-g. Kim, H. Alrowais, S. Pavlidis and O. Brand, *Adv. Funct. Mater.*, 2017, **27**, 1604466.
9 B. J. Carey, J. Z. Ou, R. M. Clark, K. J. Berean, A. Zavabeti, A. S. Chesman, S. P. Russo, D. W. Lau, Z. Q. Xu, Q. Bao, O. Kevehei, B. C. Gibson, M. D. Dickey, R. B. Kaner, T. Daeneke and K. Kalantar-Zadeh, *Nat. Commun.*, 2017, **8**, 14482.
10 S. Y. Tang, I. D. Joshipura, Y. Lin, K. Kalantar-Zadeh, A. Mitchell, K. Khoshmanesh and M. D. Dickey, *Adv. Mater.*, 2016, **28**, 604–609.
11 M. D. Bartlett, A. Fassler, N. Kazem, E. J. Markvicka, P. Mandal and C. Majidi, *Adv. Mater.*, 2016, **28**, 3726–3731.
12 A. Hirsch, H. O. Michaud, A. P. Gerratt, S. v. De Mulatier and S. P. Lacour, *Adv. Mater.*, 2016, **28**, 4507–4512.
13 M. D. Dickey, R. C. Chiechi, R. J. Larsen, E. A. Weiss, D. A. Weitz and G. M. Whitesides, *Adv. Funct. Mater.*, 2008, **18**, 1097–1104.
14 C. Ladd, J. H. So, J. Muth and M. D. Dickey, *Adv. Mater.*, 2013, **25**, 5081–5085.
15 M. R. Khan, C. Trlica and M. D. Dickey, *Adv. Funct. Mater.*, 2015, **25**, 671–678.
16 S.-Y. Tang, Y. Lin, I. D. Joshipura, K. Khoshmanesh and M. D. Dickey, *Lab Chip*, 2015, **15**, 3905–3911.
17 B. E. de Avila, P. Angsantikul, J. Li, M. Angel Lopez-Ramirez, D. E. Ramirez-Herrera, S. Thamphiwatana, C. Chen, J. Delezuk, R. Samakapiruk, V. Ramez, L. Zhang and J. Wang, *Nat. Commun.*, 2017, **8**, 272.
18 J. Hao, W. Yang, Z. Zhang and J. Tang, *Nanoscale*, 2015, **7**, 10498–10503.
19 H. Wang, X. Gu and C. Wang, *ACS Appl. Mater. Interfaces*, 2016, **8**, 9413–9422.
20 M. R. Khan, C. B. Eaker, E. F. Bowden and M. D. Dickey, *Proc. Natl. Acad. Sci. U. S. A.*, 2014, **111**, 14047–14051.
21 L. Sheng, J. Zhang and J. Liu, *Adv. Mater.*, 2014, **26**, 6036–6042.
22 J. Zhang, Y. Yao, L. Sheng and J. Liu, *Adv. Mater.*, 2015, **27**, 2648–2655.
23 R. M. Erb, H. S. Son, B. Samanta, V. M. Rotello and B. B. Yellen, *Nature*, 2009, **457**, 999–1002.
24 K. A. Mirica, F. Ilievski, A. K. Ellerbee, S. S. Shevkoplyas and G. M. Whitesides, *Adv. Mater.*, 2011, **23**, 4134–4140.
25 F. Xu, C. A. Wu, V. Rengarajan, T. D. Finley, H. O. Keles, Y. Sung, B. Li, U. A. Gurkan and U. Demirci, *Adv. Mater.*, 2011, **23**, 4254–4260.
26 J. Jeon, J. B. Lee, S. K. Chung and D. Kim, *J. Microelectromech. Syst.*, 2016, **25**, 1050–1057.
27 J. Jeon, J. B. Lee, S. K. Chung and D. Kim, *Lab Chip*, 2016, **17**, 128–133.
28 D. Kim and J.-B. Lee, *J. Korean Phys. Soc.*, 2015, **66**, 282–286.
29 J. Zhang, R. Guo and J. Liu, *J. Mater. Chem. B*, 2016, **4**, 5349–5357.
30 K. Zhang, Q. Liang, S. Ma, X. Mu, P. Hu, Y. Wang and G. Luo, *Lab Chip*, 2009, **9**, 2992–2999.
31 S. Mitsuhiro, T. Kentaro, H. Hiroyuki, I. Hiroshi and S. Kazuo, *J. Micromech. Microeng.*, 2006, **16**, 1875.
32 M. Ishii and N. Zuber, *AIChE J.*, 1979, **25**, 843–855.
33 D. Zrnic and D. S. Swatik, *J. Less-Common Met.*, 1969, **18**, 67–68.
34 J. Shao, M. Xuan, H. Zhang, X. Lin, Z. Wu and Q. He, *Angew. Chem., Int. Ed.*, 2017, **56**, 12935–12939.
35 J. Li, S. Thamphiwatana, W. Liu, B. Esteban-Fernández de Ávila, P. Angsantikul, E. Sandraz, J. Wang, T. Xu, F. Soto, V. Ramez, X. Wang, W. Gao, L. Zhang and J. Wang, *ACS Nano*, 2016, **10**, 9536–9542.
36 W. Gao, A. Uygun and J. Wang, *J. Am. Chem. Soc.*, 2012, **134**, 897–900.
37 Y. Lu, Q. Hu, Y. Lin, D. B. Pacardo, C. Wang, W. Sun, F. S. Ligler, M. D. Dickey and Z. Gu, *Nat. Commun.*, 2015, **6**, 10066.
38 Y. L. Han, H. Liu, C. Ouyang, T. J. Lu and F. Xu, *Sci. Rep.*, 2015, **5**, 11488.
39 R. K. Kramer, J. W. Boley, H. A. Stone, J. C. Weaver and R. J. Wood, *Langmuir*, 2014, **30**, 533–539.
40 D. Kim, Y. Lee, D. W. Lee, W. Choi and J. B. J. B. Lee, *2013 Transducers & Eurosensors XXVII: The 17th International Conference on Solid-State Sensors, Actuators and Microsystems (TRANSDUCERS & EUROSENSORS XXVII)*, 2013, pp. 2620–2623, DOI: 10.1109/Transducers.2013.6627343.